Quantum Entanglement Distribution for Secret Key Establishment in Metropolitan Optical Networks

Muneer Alshowkan and Khaled Elleithy
Department of Computer Science and Engineering
University of Bridgeport
Bridgeport, CT 06604, USA
malshowk@my.bridgeport.edu, elleithy@bridgeport.edu

***Abstract*— Einstein-Podolsky-Rosen (EPR) is the building block of entanglement-based and entanglement-assisted quantum communication protocols. Prior shared EPR pair and an authenticated classical channel allow two distant users to share a secret key. To build a network architecture where a centralized EPR source creates entangled states by the process of spontaneous parametric down-conversion (SPDC) then routes the states to users in different access networks. We present a metropolitan optical network (MON) architecture for entanglement distribution in a typical telecommunication infrastructure. The architecture allows simultaneous transmission of classical and quantum signals in the network and provides a dynamic routing mechanism to serve the entire MON. However, the strong launch power of the classical signals impairs the weak quantum signals when they coexist in the same optical fiber. Raman scattering Stokes-shift is the major physical impairment on the higher wavelength quantum signals which, caused by the lower wavelength classical signals. Therefore, we also study the physical impairments in the network to reduce the nonlinear effects and improve the quality of the signals. In our architecture, quantum and classical signals travel in the same optical fiber, but in different spectral bands. We show Raman Stokes-shift wavelength range and the peak power gain when simultaneous transmission of both signals occur in the same optical fiber. Reducing the physical impairments increases the traveling distance of the signals and the number of the access networks in the MON.**

***Index Terms*— architecture, security, cryptography, quantum, entanglement, qkd, epr.**

I. Introduction

Quantum information processing offers higher capacity than Shannon limit [1] and offers unconditional security [2], [3]. Quantum communication provides high capacity in optical communication by making the signals dense in the phase space so the indistinguishability of the quantum states signals becomes a matter [4]. In addition, quantum engineering introduced more advancement in the capacity [5], [6], [7], [8]. The high capacity plays an important role in the optical space long distance communication due to the lack of proper amplifiers in optical networks [9]. However, it is expected that quantum communication will mature and reach the full capacity limits [11], [12], [13]. Because tapping on classical information in fiber optic is possible, physical layer security is vulnerable to different attacks. Let alone, information leaks within the same fiber links by crosstalk and in particular when the fiber cable is bent [14]. Therefore, quantum cryptography and quantum key distribution became promising solutions for cryptography and secure data communication [15]. Following, experiments and deployments on quantum key distribution increased [18], [19], [20], [21]. As a result, the well-known BB84 protocol was the first commercialized quantum key distribution. Recent experimental deployment of a differential phase shift quantum key distribution was successful with a key rate of 1.1 kbps in a 90 km metropolitan area [19].

The motivation of our work is that two remote parties can create and exchange a secret key using the unconditional security quantum physics provides. A prior shared small secret key helps in creating an arbitrary larger one as the security of quantum cryptography is based on the laws of quantum mechanics. However, current quantum key distribution protocols are limited to symmetric-key algorithms and the point-to-point connection setups [15]. In addition, the communicating parties are required to have access to two types of communication channels. An authenticated classical channel and, an optical channel made of dedicated optical fiber links or point-to-point free-space line-of-sight [22], [23]. Migrating quantum key distribution protocols from point-to-point to many-to-many network setup requires different structure and becomes costlier [24], [18], [25], [20]. Telecommunication companies have adopted and implemented optical networking in their telecommunication networks [26]. In addition, there is an increasing interest in the passive optical networks (PON) because active components like optical amplifiers and some converters are not required. Also, its reliability and the robustness is expected to increase [27]. Thus, it is possible to have a reliable uninterrupted optical channel linking two parties for sending and receiving quantum states. Therefore, it is possible to integrate quantum channels in the telecommunication networks for commercialization [28], [29], [30], [31], [32], [33], [34], [35], [36], [37], [38], [39], [40], [41], [42]. Furthermore, having wavelength division multiplexing techniques as a standard in the telecommunication networks made optical networking infrastructure possible to serve multiple parties [43]. Specifically, quantum key distribution can use the wavelength division multiplexing (WDM) techniques to create a unique and a dedicated quantum channels [44]. However, quantum channels need to be isolated from the classical channels because quantum signals are much weaker

978-1-5090-3315-7/16/$31.00 ©2016 IEEE

TABLE I
INSERTION LOSSES IN COMMON OPTICAL NETWORK COMPONENTS

Component	Wavelength range	Insertion loss (dBm)
Single-mode fiber	1550	0.2 km
Single-mode,fiber	1310	0.32 km
CWDM mux,8-Ch	1270-1610	1.5
Switch 32,x 32	1270-1675	1

than the classical ones. Thus, the signals of quantum states are prone to be disturbed when they are traveling simultaneously with the classical signals in the same fiber optic.

In this paper, we present a MON architecture for quantum entanglement distribution and secret keys establishment. We identify and design the main components of the network. Then, we study the challenges caused by the physical impairments. Using a typical telecommunication infrastructure, our architecture provides a mechanism for simultaneous transmission of quantum and classical signals in the same optical fiber with minimum signal interference.

We also design a reconfigurable backbone node for dynamic and selective wavelength adding, passing or dropping in any access network. The architecture distributes quantum entanglement and extends the signals traveling distance. Consequently, it increases the number of the access network in the MON. Section II we cover the related work and the recent approaches in the literature. In section III we present a MON for entanglement distribution. We cover the backbone network, the access networks, the physical impairments, Raman scattering, the channels of the classical and quantum signals and, the entanglement distribution in MON. Finally, the conclusion in section IV.

II. RELATED WORK

Three designs of MON for quantum entanglement distribution were proposed in [45]. The designs had off-the-shelf MON components to decrease the overall cost and to integrate them with the current telecommunication infrastructure Table I. The access networks had tree topologies connecting many users. Two users in different access networks can receive entangled states with no restrictions on their physical locations. The first design was a single access network with direct links to distribute two entangled photons. It had low cost and low signal loss because it involved few networking components. However, it was possible to create up to eight access networks because of the utilization of the CWDM and the DWDM techniques. Other two designs were proposed for quantum applications that required conventional and quantum communication channels. One of them uses both channels and contains three access networks connected to a ring backbone topology by passive (OADM). And the other design increased the number of the access networks by using mesh topology. As a result, the communication distance increased with acceptable signal loss and the use of different paths made the network robust against attacks and link issues.

GHz-clocked QKD system is the practical design in [3] for generating and distributing entangled states. Secret key management subsystem supports different quantum applications. The design showed the true limit of QKD and provided the possible solution to realize high security for long-distance communications. In addition, it quantified the trade-off between reliability and network security, especially when taking into considering the length of the secret and the network cost. Unifying different approaches led to developing eight channels WDM. The Implementation of the design was in a network that scales a metropolitan optical network. The setup used two WDM channels with wavelengths of 1547.72nm and 1550.92nm for sending signals. And two avalanche photodiode detectors (APD) for receiving the signals. Decoyed BB84 protocol with time-bin signals showed 1.244GHz clock rate.

There are security threats arising in photonic networks. Confidentiality and integrity of the data being transmitted in the optical fiber were the focus in [24]. For example, control plane in commercial networks is a useful tool in photonic networks, especially for path control automation. However, it has a risk for controlling different network layers and its ability to open closed networks. Also, the cross-connect and the reconfigurable optical add-drop multiplexer are vulnerable to security threats. The proposed protocol provided a conceptual secure model for QKD in photonic networks. It manages the secret keys generated by QKD to encrypt user data and network control signals by KMS. And, it secures the quantum states path by working with different controllers.

Gigahertz-clocked multi-user QKD is an application of quantum cryptography over a passive optical network (PON) in [33]. It utilizes the unused wavelength of 850nm and compatible with current fiber optic telecommunication. The clock rate is up to 3 GHz and it covers MON that spans a distance of 10km. There are two approaches for the access network. First uses the middle node as a passive optical splitter to form many-to-many links. This approach reduces the network cost and complexity compared to a multi-users quantum system with dedicated links. The second approach is one-to-many PON with a typical optical splitter to transmit data in different routes. Both approaches were efficient and showed low QBER. However, the first approach can offer a higher transmission rate when finding the optimal number of photons per pulse. The second approach is susceptible to polarization-dependent loss (PDL) in the wavelength of 850 nm, which results in low bit rate. Using PDL compensator between sender and receiver reduces this effect.

III. ENTANGLEMENT DISTRIBUTION FOR SECRET KEY ESTABLISHMENT IN OPTICAL NETWORKS

In this section, we present our quantum entanglement distribution architecture. The main challenges are finding a dynamic distribution mechanism and reducing the physical impairments. Therefore, we start by presenting the backbone network and the design of the dynamic backbone nodes. Then, we define the wavelengths of the classical and the quantum communication channels. After, we study the physical impairments in the defined channels. Specifically, we study Raman scattering, which is the main physical impairment when

the launch power of the shorter wavelength classical signal is greater than the launch power of the longer wavelength quantum signal. We show the impact of Raman Stokes-shift on the signals of the quantum channel. After that, we show a simple design of entanglement distribution in an access network. Finally, we present the complete architecture and the numerical results for the entire network.

A. Backbone Network

In our design, the backbone network connects many access networks and has a ring topology. Reconfigurable optical add/drop multiplexers (ROADM) are nodes in the backbone for selective wavelength adding, dropping, or passing. Optical line terminals (OLT) are nodes at the end of point-to-point links to multiplex a set of wavelengths into a single fiber and demultiplex a set of wavelengths into multiple fibers. We are considering CWDM as the multiplexing technique in the core network, which is a typical technique in the telecommunication infrastructures. Based on the ITU standards, CWDM grid has 18 channels between 1270 nm and 1610 nm for spacing of 20 nm. We place a ROADM on the backbone for each access network and OLT between the ROADM and the access network component. The OLT does not require a transponder because all the signals will have a wavelength that matches CWDM or DWDM. ROADM handles traffic between the backbone and the access network by adding, dropping, or passing specific signals Fig. 1. We designed the ROADM using eight channels CWDM multiplexer and 32x32 Micro-electro-mechanical systems (MEMS) optical switch Fig. 2. The insertion losses of the multiplexer and the optical switch are 1.5 and 1 dBm respectively as in Table I. When the backbone traffic arrives at the ROADM, it gets demultiplexed in the backbone/ROADM to eight channels and passes to the optical switch inputs 1 to 8. If a signal does not belong to the current access network, the switch passes it to the corresponding 1 to 8 output to be multiplexed in the backbone/ROADM then passes to the backbone. Signal belonging to the access network passes to outputs 9 to 16 for multiplexing in the AN/ROADM and then passes to the access network. Access network outbound traffic gets demultiplexed in the AN/ROADM. Then, passes to the switch in the inputs 9 to 16. It gets multiplexed in the backbone/ROADM then sent to the backbone. This node introduces an insertion loss of 4 dBm for passing, dropping, or adding traffic.

B. Assignment of Quantum and Classical Channels

Applications of quantum cryptography requires two communication channels. A quantum channel to send physical quantum states and a classical channel for information reconciliation and privacy amplification. So, transmitting quantum and classical signals in the same network is important. However, in fiber-optic communication, the launch power of the classical signals is much stronger than the launch power of the quantum signals. So, nonlinear interaction occurs from Raman scattering and four-wave mixing (FWM). For this reason, the overlap between classical and quantum signals

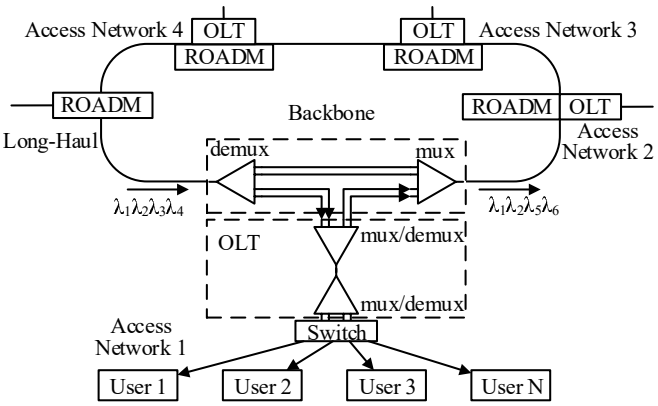

Fig. 1. This MON has four access networks. Incoming traffic from the backbone arrive to the ROADM for dropping in the access network, adding data from the access network to the backbone, or directly passing to the backbone.

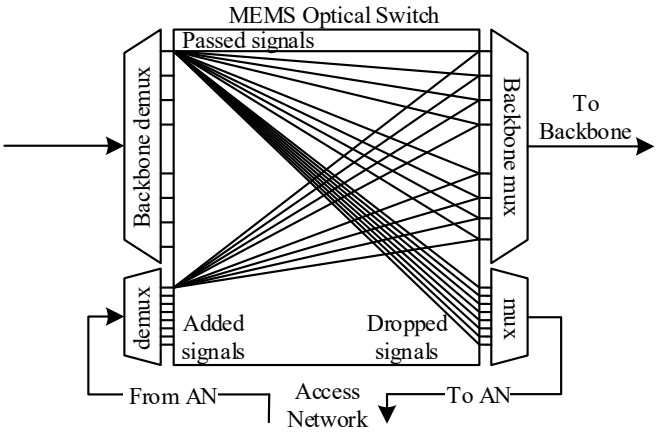

Fig. 2. ROADM is made of multiplexer/demultiplexer and MEMS optical switch. The optical switch is reconfigurable remotely to route the inputs from the demultiplexer to either the backbone for passing or the access network mux for dropping. The access network demultiplexer passes signals to the switch, which are then routed to the backbone.

become difficult to reject. Therefore, we separate the quantum and the classical signals to travel in different spectral bands. The classical signals travel in the original O-band (1260-1360). Also, the quantum signals travel within the S-band (1460-1530), C-band (1530-1565), and L-band (1565-1625). In addition, the quantum signals travel in the low loss region as the typical attenuation loss in 1300 nm is 0.4 dBm/km while in 1550 nm is 0.25 dBm/km. Based on the ITU grid standards for the CWDM, the space between channels is 20 nm. Moreover, a pair of entangled states can travel in the S-band at 1531-1571 nm and at 1511-1591 nm [46]. Consequently, entangled states can be created in DWDM or CWDM ITU channels by fine adjustments of the light source power in the SPDC process.

C. Physical Impairments

The infrastructures of optical networks can transmit a classical signal even with the existence of crosstalk. Giving that, the added noise is 40 dBm less than the launch power of the original signal. The launch power of classical channels can be

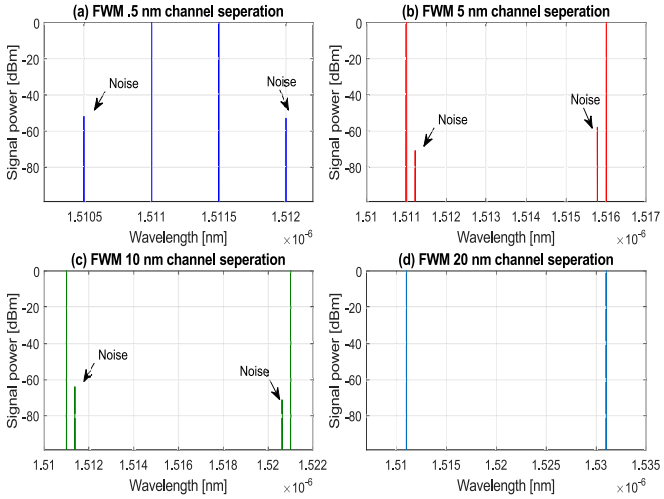

Fig. 3. Shows the FWM with respect to different separation between two continuous wave (cw) pumps with launch power of 0 dBm. Increasing the channel separation and the distance decreases the FWM effect.

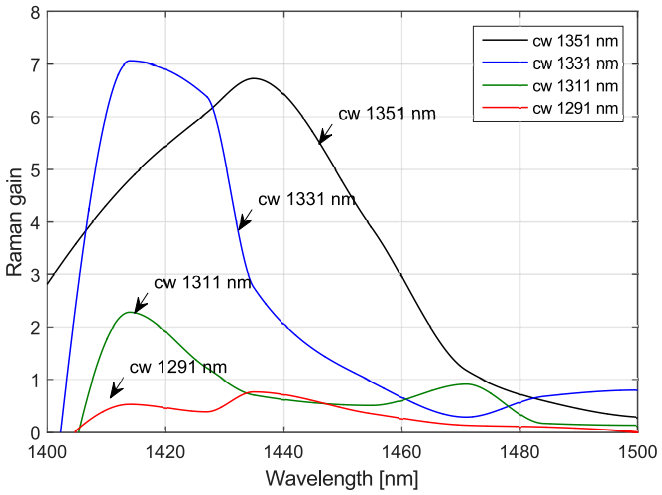

Fig. 4. Shows the range of Raman gain (in arbitrary unit) caused by the pump of the classical channels. The maximum Raman gain of the 1351 nm channel occurs at wavelength of 1435 nm. All the major noise of the classical channels occurred before the wavelengths of the quantum channels.

100 dBm greater than the launch power of the quantum signals. Therefore, classical and quantum channels react differently to the physical impairments that occur within the channels. The source of noise in the optical networks mainly arises from FWM and Raman scattering. Additionally, amplified spontaneous emission generated from optical amplifiers and weak isolation from the classical channels affect the quantum signals [47]. The Interaction in fiber optic that occurs between two or more pumps and the fiber optic X^3 nonlinearity causes the FWM. FWM produces most of the noise in short distance links when the at frequencies close to each other. However, in practice, separated frequencies and long distance links make the effect of the FWM much weaker than the effect of Raman scattering. To show the impact of FWM is not within our defined channels, we set a two continues wave pump to 0 dBm, then vary the separation between the wavelengths Fig. 3. As a result, the impact of FWM decreases and becomes very weak when the channel spacing is equal or larger than 20nm. Additionally, polarization multiplexing and improving channel configuration reduces the impact of the FWM [48]. Thus, we will examine the effects that Raman scattering has on the quantum channels.

D. Raman Scattering

In stimulated Raman scattering (SRS), the power of the lower-wavelength channels transfers to the higher-wavelength channels. The interactions between the photons change their wavelength. Subsequently, this affects other channels in the medium. Increasing or decreasing a photon energy results in generating photons with higher and lower wavelengths than the original photons are referred to as Stokes and anti-Stokes, respectively. Stimulated Brillouin scattering (SBS), which is based on the vibrational energy, has a lower effect on the quantum channel because it has a frequency shift of 10 GHz. The SBS shift is small especially for CWDM networks with a spacing grid of 20 nm. However, Raman scattering has a larger frequency shift up to 15 THz with intensity peak at 13 THz. The direction of the frequency shift caused by the flat dispersion is free from the scattering direction. Therefore, a frequency shift occurs in the directions of the propagation as well as the direction of counter propagation [49]. The Raman frequency shift is giving by:

$$hv' = hv \pm hf_v \tag{1}$$

Where hv', hv, and hf_v are the new photon energy, the incident photon energy, and the vibrational energy respectively. In our design, the classical channel at 1351 nm is closest to the quantum channel at 1531 nm. The maximum gain of Raman scattering is known to be within 13 THz from the pump signal. So, the frequency of the classical channel is:

$$\frac{3 * 10^8 m/s}{1.351 * 10^{-6} m} = 2.22 * 10^{14}\ Hz \tag{2}$$

and the stokes-shift frequency is:

$$v' = (22.2 - 1.3) * 10^{13} = 2.09 * 10^{14} \tag{3}$$

Therefore, the Stokes-shift will correspond to wavelength:

$$\lambda = \frac{3 * 10^8}{2.09 * 10^{14}} = 1435\ nm \tag{4}$$

To verify the effect of Raman Stokes-shift in our architecture we set the pumps of the classical channels to launch 0 dBm at 1351,1331,1311 and 1291 nm, then we observed the Raman scattering Stoke-shift. The maximum power gain of the classical channels 1331 and 1351 nm occurred at 1415 and 1435 nm respectively also, the peak gain power of the 1311 and 1291 nm channels occurred before at 1389 and 1367 nm respectively Fig. 4. Thus, in our design, the classical signals have a minimum effect on the quantum channels. Also, we varied the separation between the channels to observe the noise reaching the quantum signals. We varied the spacing

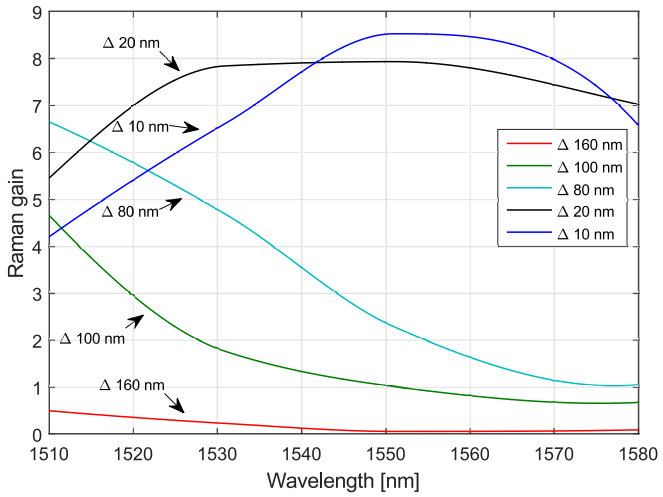

Fig. 5. Shows the noise (in arbitrary unit) caused by the classical channels as they get closer to the quantum channels. The lowest power gain occurs at highest channel separation.

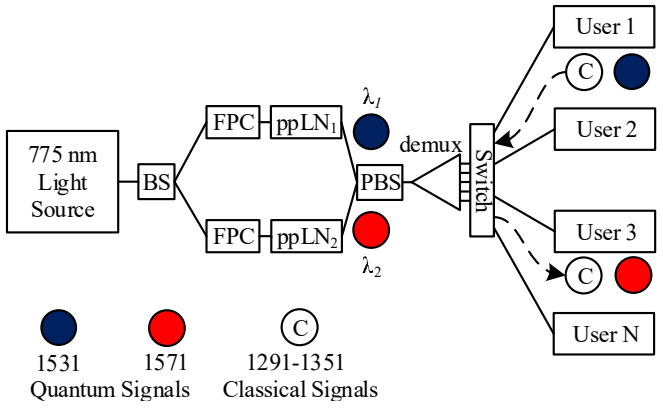

Fig. 6. This diagram illustrates the direct entanglement distribution in the access network. The output states of the process of SPDC are demultiplexed and sent to the optical network switch, then to the end users. Classical communication signals between users are routed through the optical switch.

between the highest classical channel wavelength (1351 nm) and the lowest quantum channel wavelength (1511 nm). We notice that the noise in the quantum channels increases as the classical channel get closer to the quantum signals Fig. 5. Therefore, in our architecture, Raman Stokes-shift from the classical channels has less impact on the quantum channels.

E. Entanglement Distribution in an Optical Access Network

Let us consider entanglement distribution and classical communication in an access network. The EPR source, which is located in the access network, have direct communication with all users through the optical network switch. Using laser with pump power of -99 dBm, we setup the wavelength of the laser in the SPDC to create two entangled states set at 1531 nm and 1571 nm Fig. 6. A WDM multiplexer carries the signals from the EPR source to the network switch. Then, the switch forwards the entangled states to the end users. The insertion losses in the CWDM multiplexer and the optical switch are 1.5 dBm/km and 1 dBm, respectively. This results in a slight decrease in the coincidence rates [46]. We used the O-band between 1271 nm and 1351 nm for the classical communication. The extra connections in the optical switch routes the classical communication between the users [45] within the access network. Since this access network has a short distance with few components, it has a low insertion loss close to 3 dBm.

F. Entanglement in Metropolitan Optical Network

We based the core network on ITU-T G.694.2 CWDM that contains a grid wavelength range between 1270 nm and 1610 nm. This spectral grid has 18 channels based on a space of 20 nm between the channels. We designate the wavelengths between 1271 nm and 1351 nm for the classical communication which launches signals at power of 0 dBm. Also, the wavelengths 1511 nm and 1571 for the quantum communications. We setup the EPR source as a centralized node for entanglement distribution in the entire MON. Users in the same or different access networks requests to share entanglement pairs for establishing secret keys using entanglement-based and entanglement-assisted quantum key distribution. When the EPR source receives a request, it creates entangled states by the process of SPDC in 1531-1571 nm or 1511-1551 nm, which correspond to CWDM channels. The output states travel from the EPR access network to the CWDM based backbone via the local ROADM. Then, the EPR source remotely reconfigures the MEMS optical switches in the ROADMs to drop the wavelengths of the entangled states in the target access networks. Then, they pass through the AN/ROADM multiplexer. Then, the signals are demultiplexed to the network switch. Finally, the optical switch transmits the states to the end users Fig. 7. Using the dedicated and authenticated classical channel of each access network, users establishes secret keys using quantum key distribution protocols.

In the MON, we assume that the distance between neighboring backbone nodes is 4 km and the distance between the backbone node and the access network switch is 3.5 km. Also, we assume that the distance between the access network switch and the end users is 1 km. We estimate the insertion loss in the network based on loss budget of 30 dBm [36]. Each access network has different insertion loss because of the centralized EPR source. The major insertion loss in the first access network results from two backbone nodes, fiber optic attenuation, and the access network switch. Therefore, the total insertion loss in the first access network is 13.22 and 10.6 dBm for the classical and quantum channels respectively. In the second access network, the signals travel through three backbone nodes and double the distance of the first access network. The total insertion loss of the second access network is 18.5 and 15.4 dBm for classical and quantum channels respectively. The insertion loss for the entire access network in the MON is provided in Table II.

The maximum insertion loss occurs in the fourth access network as the signals travel the longest distance and pass

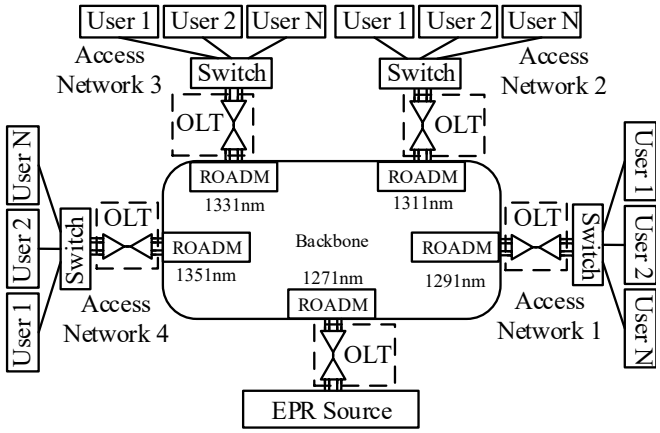

Fig. 7. This diagram shows the centralized EPR source for entanglement distribution in MON. Quantum signals sent from the EPR travel in the backbone network then dropped in the designated access network by the ROADM. By remotely reconfiguring the optical switches in the ROADM causes the wavelength of the entangled state to pass or drop. The wavelength of the classical channel is fixed for each access network and used for the classical communication between the users in different access networks.

TABLE II
INSERTION LOSS FOR EVERY ACCESS NETWORK IN MON

Network	No. ROADM	Loss C ch (dBm)	Loss Q ch (dBm)
AN-1	2	13.22	10.6
AN-2	3	18.5	15.4
AN-3	4	23.78	20.2
AN-4	5	29.06	25

through several backbone nodes. The largest insertion loss in this network is tolerable as it falls below the acceptable 30 dBm loss budget. Adding new access networks results in insertion loss greater than 30 dBm in the new access networks. However, increasing the number of the users in each access network has no effect on the insertion loss of the access networks. Consequently, the overall performance of the network remains unchanged. In Fig. 8 we show the optical noise

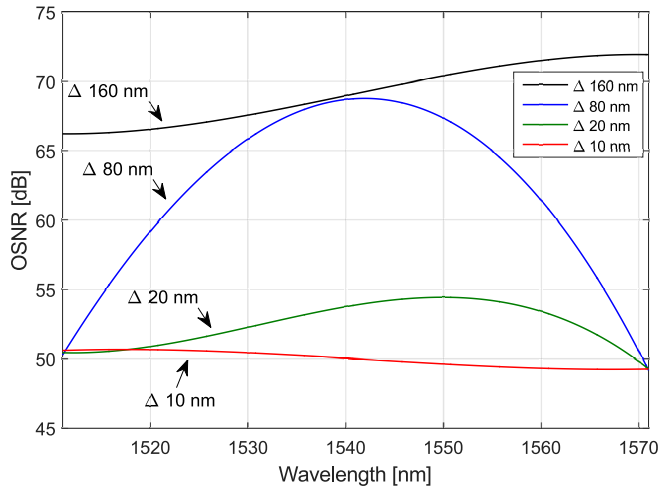

Fig. 8. Shows the optical signal-to-noise ratio in the quantum channels with respect to different spacing to the wavelength of the classical signals.

to signal ration (ONSR) with respect to a different channel spacing between the classical and the quantum channels. The spacing in our architecture proves better ONSR because the classical signals have less impact on the quantum channels. Fig. 9 shows the power of the signals measured at the last access network for fiber lengths of 20,40 and, 80 km.

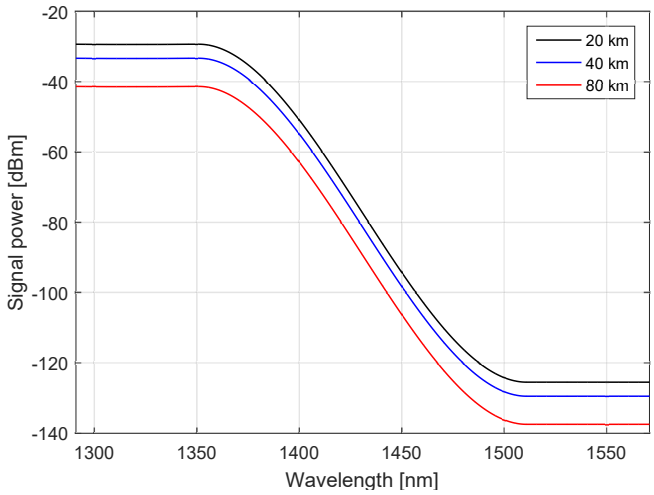

Fig. 9. Shows the power of the signals of the classical and the quantum channels at the last access network and under different 20, 40 and, 80 km fiber length. Note that, the drop between 1351 nm to 1511 nm indicates the spacing between the classical and the quantum channels.

Also, we show the bit error rate in Fig. 10 with respect to the length of the fiber optic. The fiber attenuation loss decreases the signal power which increases the bit error rate. It is possible to amplify the classical signal to reduce the BER and increase the signals traveling distance. However, there is no equivalent quantum amplifier quantum due to the no-cloning theorem [50].

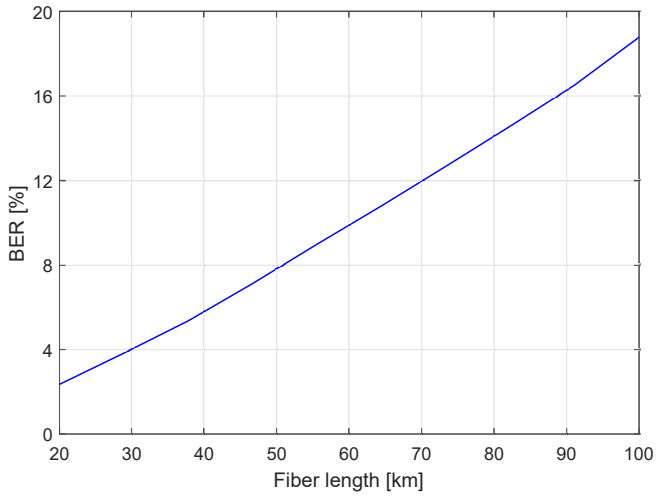

Fig. 10. Shows the bit error rate of the classical channels for fiber length between 20 and 100 km.

We compare our network with the reference work in [45] using the same parameters in Table I. We reduced the overall

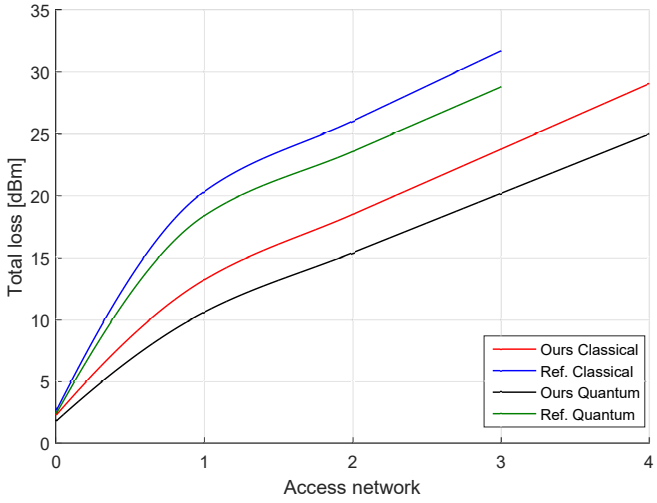

Fig. 11. Shows comparison between our network and the reference work. We reduced the network loss and increased the number of access networks from three to four within the acceptable network signal loss.

network loss and increased the number of the access networks from three to four Fig. 11. Also, we considered a centralized EPR source to serve the entire MON instead of local EPR sources. The design of our ROADM provides a dynamic adding, dropping, or passing of the quantum wavelengths at each backbone node. In addition, the assigned classical channel provides a private communication between the access networks.

IV. CONCLUSION

In this paper, we presented a quantum entanglement distributing entangled in metropolitan optical networks. The centralized entanglement source serves all the users in the network. It creates entangled pairs with wavelengths that correspond to channels in the CWDM. By specifying the wavelengths to drop, or pass at each backbone node, we provided a dynamic entanglement distribution for the entire network. Quantum and classical signals travel in the same fiber optic within different spectral bands. Classical signals travel within the range of 1271 nm and 1351 nm while quantum signals travel within the range of 1531 nm and 1571 nm. We reduced the effect of Raman gain caused by the classical channels at the wavelengths of the quantum channels. The maximum insertion loss in the network is 25 and 29 dBm for the quantum and the classical channels respectively, which falls below the acceptable 30 dB budget loss.

REFERENCES

[1] C. E. Shannon, "A mathematical theory of communication," *Bell System Technical Journal*, vol. 5, no. 1, pp. 379–423, 1947.

[2] A. Abeyesinghe *et al.*, "Generalized remote state preparation: Trading cbits, qubits and ebits in quantum communication," *Physical Review A*, vol. 68, no. December, p. 15, 2003.

[3] M. Sasaki *et al.*, "Quantum photonic network: Concept, basic tools, and future issues," *IEEE Journal on Selected Topics in Quantum Electronics*, vol. 21, no. 3, pp. 49–61, 2015.

[4] A. Waseda *et al.*, "Quantum detection of wavelength division multiplexing optical coherent signals," *JOSA B*, vol. 27, no. 2, pp. 259–265, 2010.

[5] M. Fujiwara *et al.*, "Exceeding the classical capacity limit in a quantum optical channel." *Physical review letters*, vol. 90, no. 16, p. 167906, 2003.

[6] M. Sasaki *et al.*, "A demonstration of superadditivity in the classical capacity of a quantum channel," *Physics Letters A*, vol. 236, no. 1-2, pp. 1–4, 1997.

[7] M. Sasaki *et al.*, "Quantum channels showing superadditivity in capacity," *Phys. Rev. A*, vol. 58, no. 1, p. 16, 1998.

[8] M. Takeoka *et al.*, "Implementation of generalized quantum measurements: Superadditive quantum coding, accessible information extraction, and classical capacity limit," *Physical Review A - Atomic, Molecular, and Optical Physics*, vol. 69, no. 5 A, pp. 052 329–1, 2004.

[9] a. Waseda *et al.*, "Numerical Evaluation of PPM for Deep-Space Links," *IEEE/OSA Journal of Optical Communications and Networking*, vol. 3, no. 6, pp. 514–521, 2011.

[10] V. Giovannetti *et al.*, "Classical capacity of the lossy bosonic channel: the exact solution." *Physical review letters*, vol. 92, no. 2, p. 027902, 2004.

[11] P. Hausladen *et al.*, "Classical information capacity of a quantum channel," *Physical Review A*, vol. 54, no. 3, pp. 1869–1876, 1996.

[12] A. S. Holevo, "The capacity of the quantum channel with general signal states," *IEEE Transactions on Information Theory*, vol. 44, no. 1, pp. 269–273, 1998.

[13] B. Schumacher *et al.*, "Sending classical information via noisy quantum channels," *Physical Review A*, vol. 56, no. 1, pp. 131–138, 1997.

[14] M. Fujiwara *et al.*, "Photon level crosstalk between parallel fibers installed in urban area." *Optics express*, vol. 18, no. 21, pp. 22 199–22 207, 2010.

[15] C. H. Bennett *et al.*, "Quantum cryptography," *Sci. Am.*, vol. 267, no. (4), pp. 50–57, 1992.

[16] J. F. Dynes *et al.*, "Stability of high bit rate quantum key distribution on installed fiber," *Optics Express*, vol. 20, no. 15, p. 16339, 2012.

[17] C. Elliott *et al.*, "Current status of the DARPA Quantum Network," in *Proc. SPIE 5815, Quantum Information and Computation III,*, vol. 5815. International Society for Optics and Photonics, 2005, pp. 138–149.

[18] M. Peev *et al.*, "The SECOQC quantum key distribution network in Vienna," *New J. Phys.*, vol. 11, no. 7, p. 75001, 2009.

[19] K. Shimizu *et al.*, "Performance of Long-Distance Quantum Key Distribution Over 90-km Optical Links Installed in a Field Environment of Tokyo Metropolitan Area," *Lightwave Technology, Journal of*, vol. 32, no. 1, pp. 141–151, 2013.

[20] D. Stucki *et al.*, "Long-term Performance of the Swiss Quantum Quantum Key Distribution Network in a Field Environment," *New Journal of Physics*, vol. 13, no. 12, pp. 1–18, 2011.

[21] K.-i. Yoshino *et al.*, "Maintenance-free operation of WDM quantum key distribution system through a field fiber over 30 days," *Optics Express*, vol. 21, no. 25, p. 6, 2013.

[22] P. Jouguet *et al.*, "Field Test of Classical Symmetric Encryption with Continuous Variable Quantum Key Distribution," *Optics Express*, vol. 10387, no. 13, p. 14030, 2012.

[23] A. Mirza *et al.*, "Realizing long-term quantum cryptography," *Journal of the Optical Society of America B*, vol. 27, no. 6, p. A185, 2010.

[24] K. I. Kitayama *et al.*, "Security in photonic networks: Threats and security enhancement," *Journal of Lightwave Technology*, vol. 29, no. 21, pp. 3210–3222, 2011.

[25] M. Sasaki *et al.*, "Field test of quantum key distribution in the Tokyo QKD Network," *Optics Express*, vol. 19, no. 11, p. 10387, 2011.

[26] Y. Chen *et al.*, "Metro optical networking," *Bell Labs Technical Journal*, vol. 4, no. 1, pp. 163–186, 1999.

[27] C. H. Lee *et al.*, "Fiber to the home using a PON infrastructure," *Journal of Lightwave Technology*, vol. 24, no. 12, pp. 4568–4583, 2006.

[28] S. Aleksic *et al.*, "Quantum Key Distribution Over Optical Access Networks," in *Proceedings of the 2013 18th European Conference on Network and Optical Communications & 2013 8th Conference on Optical Cabling and Infrastructure (NOC-OC&I)*, 2013, pp. 11–18.

[29] J. Capmany *et al.*, "Analysis of Passive Optical Networks for Subcarrier Multiplexed Quantum Key Distribution," *Microwave Theory and Techniques, IEEE Transactions on*, vol. 58, no. 11, pp. 3220–3228, 2010.

[30] I. Choi *et al.*, "Quantum key distribution on a 10Gb/s WDM-PON." *Optics express*, vol. 18, no. 9, pp. 9600–9612, 2010.

[31] I. Choi *et al.*, "Quantum information to the home," *New Journal of Physics*, vol. 13, no. 6, p. 063039, 2011.

[32] D. Elkouss *et al.*, "Secure optical networks based on quantum key distribution and weakly trusted repeaters," *Optical Communications and Networking, IEEE/OSA Journal of*, vol. 5, no. 4, pp. 316–328, 2013.

[33] T. Buller, "Passive Optical Network Approach to Gigahertz-Clocked Multiuser Quantum Key Distribution," *Quantum Electronics, IEEE Journal of*, vol. 43, no. 2, p. 9, 2007.
[34] R. J. Hughes *et al.*, "Quantum key distribution over a 48 km optical fibre network," *Journal of Modern Optics*, vol. 47, no. 2-3, pp. 533–547, 2000.
[35] P. D. Kumavor *et al.*, "Comparison of Four Multi-User Quantum Key Distribution Schemes Over Passive Optical Networks," *Lightwave Technology, Journal of*, vol. 23, no. 1, pp. 268–276, 2005.
[36] D. Lancho *et al.*, *Q K D in Standard Optical Telecommunications Networks*. Springer, 2010, pp. 1–5.
[37] W. Maeda *et al.*, "Technologies for Quantum Key Distribution Networks Integrated With Optical Communication Networks," *IEEE Journal of Selected Topics in Quantum Electronics*, vol. 15, no. 6, pp. 1591–1601, 2009.
[38] J. Martinez-Mateo *et al.*, "Quantum Key Distribution Based on Selective Post-Processing in Passive Optical Networks," *IEEE Photonics Technology Letters*, vol. 26, no. 9, pp. 881–884, 2014.
[39] M. Razavi, "Multiple-Access Quantum Key Distribution Networks," *IEEE Trans. Commun.*, vol. 60, no. 10, pp. 3071–3079, 2012.
[40] P. D. Townsend, "Quantum cryptography on multiuser optical fibre networks," *Nature*, vol. 385, no. 6611, pp. 47–49, 1997.
[41] P. Townsend, "Experimental investigation of the performance limits for first telecommunications-window quantum cryptography systems," *IEEE Photonics Technology Letters*, vol. 10, no. 7, pp. 1048–1050, 1998.
[42] P. Townsend *et al.*, "Design of quantum cryptography systems for passive optical networks," *Electronics Letters*, vol. 30, no. 22, p. 1875, 1994.
[43] G. P. Ryan, "Dense wavelength division multiplexing networks," *IEEE Journal on Selected Areas in Communications*, vol. 8, no. 6, p. 23, 1997.
[44] A. Ciurana *et al.*, "Quantum Metropolitan Optical Network based on Wavelength Division Multiplexing," *Optics express*, vol. 22, no. 2, p. 23, 2013.
[45] A. Ciurana *et al.*, "Entanglement distribution in optical networks," *Selected Topics in Quantum Electronics, IEEE Journal of*, vol. 21, no. 3, pp. 37–48, may 2015.
[46] I. Herbauts *et al.*, "Demonstration of active routing of entanglement in a multi-user network," *Optics Express*, vol. 21, no. 23, pp. 29 013–29 024, 2013.
[47] N. A. Peters *et al.*, "Dense wavelength multiplexing of 1550 nm QKD with strong classical channels in reconfigurable networking environments," *New Journal of Physics*, vol. 11, no. 4, p. 45012, 2009.
[48] B. Qi *et al.*, "Feasibility of quantum key distribution through a dense wavelength division multiplexing network," *New Journal of Physics*, vol. 12, no. 10, p. 103042, 2010.
[49] P. Eraerds *et al.*, "Quantum key distribution and 1 Gbit/s data encryption over a single fibre," *New Journal of Physics*, vol. 12, no. 6, p. 9, 2009.
[50] W. K. Wootters *et al.*, "A single quantum cannot be cloned," *Nature*, vol. 299, no. 5886, pp. 802–803, oct 1982.